Dynamic control over feedback regulation improves stationary phase fluxes in engineered *E. coli.*

Shuai Li[1,*], Zhixia Ye[2,*], Juliana Lebeau [2], Eirik A. Moreb [2],and Michael D. Lynch [2,3,+]

[1]Department of Chemistry, Duke University

[2] Department of Biomedical Engineering, Duke University

*Authors contributed equally to this work.

[3] To whom all correspondence should be addressed.

+michael.lynch@duke.edu

Abstract: We demonstrate the use of two-stage dynamic metabolic control to manipulate feedback regulation in central metabolism and improve biosynthesis in engineered *E. coli.* Specifically, we report the impact of dynamic control over two central metabolic enzymes: citrate synthase, and glucose-6-phosphate dehydrogenase, on stationary phase fluxes. Firstly, reduced citrate synthase levels lead to a reduction in α-ketoglutarate, which is an inhibitor of sugar transport, resulting in increased glucose uptake and glycolytic fluxes. Reduced glucose-6-phosphate dehydrogenase activity activates the SoxRS regulon and expression of pyruvate-ferredoxin oxidoreductase, which is in turn responsible for large increases in acetyl-CoA production. These two mechanisms lead to the improved stationary phase production of citramalic acid enabling titers of 126±7g/L. These results identify pyruvate oxidation via the pyruvate-ferredoxin oxidoreductase as a "central" metabolic pathway in stationary phase and highlight the potential of improving fluxes by manipulating essential central regulatory mechanisms using two-stage dynamic metabolic control.

Keywords: dynamic metabolic control, feedback regulation, metabolic valves, CRISPR, controlled proteolysis, glucose uptake, acetyl-CoA

Highlights:

- Dynamic reduction in α-keto-glutarate pools alleviate inhibition of PTS dependent transport improving stationary phase sugar uptake.
- Dynamic reduction in glucose-6-phosphate dehydrogenase activates pyruvate flavodoxin/ferredoxin oxidoreductase and improves stationary acetyl-CoA flux.
- Pyruvate flavodoxin/ferredoxin oxidoreductase is responsible for large stationary phase acetyl-CoA fluxes under aerobic conditions.
- Production of citramalate to titers 126 ± 7g/L at > 90 % of theoretical yield

Introduction

Biotechnology based fermentation processes have made rapid advancements in recent years due to technology developments in the fields of fermentation science and synthetic biology, as well as metabolic and enzyme engineering.(Jarboe et al. 2010; Lee et al. 2012) However improvements in rates, titers and yields are often needed to enable commercially competitive processes. Most metabolic engineering strategies aimed at improving these metrics rely on the overexpression of desired pathway enzymes and deletion and/or downregulation of competing biochemical activities. Over the last several decades, stoichiometric models of metabolism have helped to move the field from manipulating gene expression levels to manipulating networks, which can now be designed to couple growth with product formation, and selection can be used to optimize for both. (Bordbar et al. 2014; Burgard, Pharkya, and Maranas 2003)

A remaining limitation of these approaches are the metabolic boundary conditions required for cellular growth. Dynamic metabolic control and specifically two-stage control offer a potential engineering strategy to overcome these limitations, by switching to a production state where metabolite and enzyme levels can be pushed past the boundaries required for growth. (Lynch 2016; Burg et al. 2016; Brockman and Prather 2015a, [b] 2015; Venayak et al. 2018; Solomon, Sanders, and Prather 2012; Lalwani, Zhao, and Avalos 2018) Significant efforts have been made to develop tools for dynamic metabolic control including control systems, metabolic valves and modeling approaches. (Lynch 2016; Burg et al. 2016; Brockman and Prather 2015a, [b] 2015; Venayak et al. 2018; Solomon, Sanders, and Prather 2012; Lalwani, Zhao, and Avalos 2018; Gardner, Cantor, and Collins 2000; David, Nielsen, and Siewers 2016; Xu et al. 2014) However to date, previous work has largely focused on dynamically redirecting fluxes by switching "OFF" pathways that stoichiometrically compete with a desired pathway. (Brockman and Prather 2015b) In this work, we demonstrate increased stationary phase flux attributable to dynamic reduction in metabolites which act as feedback regulators of central metabolism, and not reductions in competing metabolic pathways.

As illustrated in Figure 1a, we investigate the impact of dynamic control of two central metabolic pathways (the tricarboxylic acid (TCA) cycle and pentose phosphate pathway (PPP)) on flux through glycolysis and pyruvate oxidation. We accomplish this by creating synthetic metabolic valves, (Brockman and Prather 2015a; Lynch 2016; Burg et al. 2016; Kildegaard et al. 2019; Ding, Zhang, and Shi 2020) to dynamically reduce levels of the first committed step in each pathway, namely citrate synthase (GltA, "G", encoded by the *gltA* gene) and glucose 6-phosphate dehydrogenase (Zwf, "Z", encoded by the *zwf* gene). We show that dynamic control over these two enzymes improves stationary phase production of pyruvate, and citramalate, and have applicability in the production of numerous products requiring pyruvate and/or acetyl-CoA.

Results

We first developed control systems capable of the dynamic reduction of protein levels in two-stage processes, as illustrated in Figure 1b-d. Valves rely on controlled proteolysis or CRISPRi/Cascade based gene silencing or both proteolysis and silencing in combination to reduce levels of key metabolic enzymes.(Qi et al. 2013; Luo et al. 2015a; McGinness, Baker, and Sauer 2006; Lynch 2016; Burg et al. 2016) Induction is implemented using phosphate depletion as an environmental trigger.(Romel Menacho-Melgar et al., n.d.; R. Menacho-Melgar, Moreb, and Efromson 2020; Huber et al. 2011; Chubukov and Sauer 2014) The native *E. coli* Type I-E Cascade/CRISPR system is used for gene silencing (Figure 1c).(Luo et al. 2015a; Brouns et al. 2008) Targeted proteolysis is implemented by linking the expression of the chaperone SspB to phosphate deprivation. SspB, when induced, binds to C-terminal DAS+4 peptide tags on any target protein and causes degradation by the ClpXP protease of *E. coli* (Figure 1d). (McGinness, Baker, and Sauer 2006) Refer to Supplemental Tables for strains and plasmids used in this study. Using engineered strains, as Figure 1e demonstrates, protein levels can be controlled in a two-stage process, as exemplified by turning "ON" GFP and "OFF" constitutively expressed (Davis, Rubin, and Sauer 2011) mCherry. While, in this case, the combination of gene silencing with proteolysis results in the largest rates of protein degradation (Figure 2f and g), the impact of each approach and specific decay rates, will vary depending on the target gene/enzyme and its

specific natural turnover rates and expression levels. (Hintsche and Klumpp 2013; Grünenfelder et al. 2001)

We then turned to dynamically reduce levels of GltA and Zwf (Figure 1h-i). We engineered strains with chromosomal modifications that appended C-terminal DAS+4 degron tags to these genes. In addition, we engineered several strains to have C-terminal superfolder GFP tags behind each gene with and without C-terminal degron tags. (McGinness, Baker, and Sauer 2006; Pédelacq et al. 2006) Plasmids expressing gRNAs were designed to repress expression from the *gltAp2* and *zwf* promoters. Using these strains and plasmids, dynamic control over enzyme levels were monitored by tracking GFP via an ELISA assay in two-stage minimal media micro-fermentations as reported by Moreb et al. (Eirik Adim Moreb et al. 2020) An ELISA was used as protein levels were too low in engineered strains to use GFP fluorescence as a direct reporter. In the case of GltA proteolysis and silencing resulted in a 70% and 85% decrease in GltA levels, respectively, with the combination resulting in a 90% reduction. In the case of Zwf, proteolysis, silencing as well as the combination all resulted in protein levels below the limit of quantification of our assay.

The impact of "G" and "Z" valve combinations on metabolic fluxes were measured in minimal media micro-fermentations, (Eirik Adim Moreb et al. 2020) performed without any heterologous production pathway. As the strains used had deletions in the major pathways leading to acetate production (*poxB,* and *pta-ackA*), pyruvate synthesis was initially evaluated as a measure of metabolic fluxes through glycolysis (Figure 2). The "G" valve had the largest impact on pyruvate production, with no detectable product measured in a control strain without SMVs. The improved production of pyruvate could be attributable either to a stoichiometric effect, wherein a portion of flux normally entering the TCA cycle is redistributed to the overflow metabolite, or alternatively to a more global increase in the sugar uptake rate enabling greater overflow metabolism and pyruvate synthesis. To evaluate these two alternatives we measured the impact of the "G" valve on glucose uptake rates. Results, shown in Figure 2c, indicate that increases in pyruvate production are primarily attributed to increases in uptake rates rather than a repartitioning of basal fluxes.

We hypothesized increased sugar uptake due to the "G" valves was due to a direct regulatory effect of metabolites produced by the TCA cycle, namely α- ketoglutarate (αKG). αKG, a precursor to glutamic acid, has several key regulatory roles,(Huergo and Dixon 2015; Rabinowitz and Silhavy 2013; Doucette et al. 2011) including the regulation of sugar transport by direct inhibition of Enzyme I of the PTS dependent glucose transporter (Figure 1). This feedback regulation is a way to coordinate sugar uptake with nitrogen assimilation (glutamate synthesis).(Doucette et al. 2011) To test our hypothesis, we performed supplementation experiments, spiking 20mM dimethyl-αKG (DM-αKG) into microfermentations at the onset of production.(Doucette et al. 2011) DM-αKG , rather than αKG was used as it has been shown to better cross the membrane, and after hydrolysis add to the intracellular αKG pool.(Doucette et al. 2011) As seen in Figure 2, DM-αKG inhibited sugar uptake in control cells as well as in strains with valves reducing GltA levels. Together these results support dynamic reduction in GltA levels and the subsequent reduction in αKG pools as primarily responsible for improved sugar uptake rates and pyruvate biosynthesis. We next turned to assess pyruvate production in instrumented bioreactors. Minimal media fed batch fermentations were performed as previously reported by Menacho-Melgar et al., (Romel Menacho-Melgar et al., n.d.) where phosphate concentration limited biomass levels and once consumed expression of the silencing gRNAs and the SspB chaperone are induced. Results comparing the control host strain with a strain having dynamic control over GltA levels are given in Figure 2d. Minimal pyruvate transiently accumulated in the control strain whereas maximal titers of over ~ 30g/L were obtained using dynamic control.

To assess the impact of dynamic control over acetyl-CoA fluxes we leveraged citramalate synthase which produces one mole of citramalate from one mole of pyruvate and one mole of acetyl-CoA (Figure 5a).(Romel Menacho-Melgar et al., n.d.; Eirik A. Moreb et al. 2020) Citramalate is a precursor to the industrial chemicals itaconic acid and methyl methacrylate, as well as an intermediate in branched chain amino acid biosynthesis.(Lebeau, Efromson, and Lynch 2020; Howell, Xu, and White 1999; Parimi et al. 2017; Wu and Eiteman 2016; J. P. Webb et al. 2018; J. Webb et al. 2019) To produce citramalate, we used a low phosphate inducible plasmid expressing a previously reported feedback resistant mutant citramalate synthase

(cimA3.7).(Atsumi and Liao 2008; J. P. Webb et al. 2018; Romel Menacho-Melgar et al., n.d.) This plasmid was introduced into the set of "G" and "Z" valve strains which were then assessed for citramalate production in two stage micro-fermentations (Figure 3). The best producing strain had both "G" and "Z" valves.

In the case of pyruvate, the "Z" valve had no significant impact on production (Figure 2b). Citramalate and pyruvate are similar products in that they are both oxidized and require no redox cofactor (such as NADPH) for biosynthesis. A key difference in the two products is that citramalate requires an additional precursor, namely acetyl-CoA. We hypothesized that the "Z-valve" dependent improvement in citramalate production was dependent on improved acetyl-CoA production in strains with reduced Zwf activity. If correct, this would suggest that either Zwf levels or the levels of downstream metabolites have a negative regulatory impact on stationary phase acetyl-CoA synthesis. It is important to note that the strains used for pyruvate and citramalate production have deletions in *poxB* and *pflB* (which can lead to acetyl-CoA synthesis) and initially we had assumed all acetyl-CoA flux was through the well characterized pyruvate dehydrogenase (PDH) multienzyme complex.(de Kok et al. 1998; Hennig et al. 1997) To our surprise, proteolytic degradation of Lpd (a subunit of PDH) had no impact on citramalate production. Based on the this we turned to consider the potential of an alternative primary route for acetyl-CoA production in stationary phase cultures, namely pyruvate-flavodoxin/ferredoxin oxidoreductase (Pfo), encoded by the *ydbK* gene.

We hypothesized, as illustrated in Figure 1, that Pfo (*ydbK*) was in part responsible for acetyl-CoA synthesis in stationary phase and that due to its role in the oxidative stress response this activity was regulated by intermediates in the PPP, also known to be involved in the response to oxidative stress.(Griffith and Wolf 2001; Greenberg et al. 1990; Christodoulou et al. 2018) To test this hypothesis we constructed a *ydbK* deletion in the citramalate strain containing both "G" and "Z" valves and measured citramalate production. As seen in Figure 3b, the deletion of *ydbK* significantly reduced citramalate synthesis confirming the role of Pfo in acetyl-CoA flux. As Pfo has been shown to be induced upon oxidative stress, via the SoxRS regulon (which is regulated by oxidant levels and NADPH pools),(Nakayama et al. 2013; Blaschkowski et al. 1982; Akhtar, Kalim Akhtar, and Jones 2009; Fàbrega et al. 2012) we hypothesize that

expression is due to alterations in NADPH levels caused by reductions in Zwf activity. Previous work has shown a modest activation of SoxRS in response to a *zwf* deletion, (Gaudu, Dubrac, and Touati 2000), and an impaired response to oxidative stress, (Giró, Carrillo, and Krapp 2006) which may be magnified by a rapid dynamic reduction on Zwf activity.

Lastly, we evaluated citramalate production strains in instrumented bioreactors. The control strain made reasonable citramalate titers (~40g/L), whereas the introduction of SMVs improved production. The combined "GZ" valve strain had the highest citramalate production, reaching titers of ~100 g/L. This process was then intensified, by increasing biomass levels from ~ 10gCDW/L to ~ 25gCDW/L, leading to titers of 126+/-7g/L. This process is illustrated in Figure 3c. Refer to Supplemental Figure S9 for the time courses for additional fermentations. The overall process yields were 0.74-0.77g citramalate/g glucose and during the production phase yields approached theoretical achieving 0.80-0.82 g citramalate/g glucose. The theoretical yield for citramalate from glucose is 1 mole/mole or 0.817g/g.

Discussion

Previous studies utilizing dynamic control have primarily been informed by a stoichiometric framework, wherein pathways are switched "ON" and "OFF" to reduce fluxes that stoichiometrically compete for a desired product, or in other words pathway redirection.(Brockman and Prather 2015b; Maury et al. 2018) For example Venayak and colleagues (Venayak et al. 2018) have highlighted the importance of GltA/CS as a central valve candidate for dynamic metabolic control, based in part on stoichiometric modelling. (Soma et al. 2014; Venayak et al. 2018) However these studies and models have missed the importance of the regulatory role of downstream metabolites, such as αKG. This work demonstrates that increasing flux by dysregulation of feedback control can have a large impact on production, independent of stoichiometry or the minimization of competing pathways. In particular, it was unexpected that reducing Zwf activity increases acetyl-CoA fluxes.

To our knowledge this is the first report of the interaction between minimal Zwf levels, SoxRS activation and Pfo activity in stationary phase. Additionally, the magnitude of the metabolic flux through Pfo is unexpected. Although Pfo, an iron sulfur cluster containing

enzyme, has been successfully expressed in both aerobic and anaerobic conditions, (Akhtar, Kalim Akhtar, and Jones 2009; Nakayama et al. 2013; Eremina 2010; Fàbrega et al. 2012) it is quickly inactivated by molecular oxygen *in vitro,* and as a result, conventional wisdom would suggest it is unlikely to support these types of fluxes. (Blaschkowski et al. 1982; Nakayama et al. 2013) These data suggest that the Pfo pathway can operate as a central metabolic pathway under certain conditions, and that high levels of activity can be maintained even aerobically *in vivo.* More work is needed to understand the mechanisms underlying the observed *in vivo* oxygen tolerance of this pathway. Improved understanding may lead to alternative strategies (independent of decreasing Zwf levels) for optimizing fux through this pathway, such as pathway overexpression and/or enzyme engineering.

More generally, this work highlights the potential of manipulating known and unknown feedback regulatory mechanisms to improve *in vivo* enzyme activities and metabolic fluxes. This approach can open numerous novel engineering strategies, and has the potential to lead to significant improvements in production rates, titers and yields. Furthermore these results confirm the metabolic potential of stationary phase cultures.(Burg et al. 2016; Romel Menacho-Melgar et al., n.d.; Lynch 2016; Chubukov and Sauer 2014) Dynamic metabolic control in two-stage cultures is uniquely suited to implement these strategies. Simply overexpressing key enzymes does not bypass native regulation and the complete removal of central metabolic enzymes and/or metabolites will often lead to growth defects and strains which need to evolve compensatory metabolic changes to meet the demands of growth. In contrast changes to levels of central regulatory metabolites in stationary phase enable rewiring of the regulatory network and metabolic fluxes without this constraint. (Burg et al. 2016; Lynch 2016)

Methods

Media & Reagents

Unless otherwise stated, all materials and reagents were purchased from Sigma (St. Louis, MO). Luria Broth Lennox formulation was used for routine strain and plasmid propagation and construction. FGM1, FGM30, and SM10++ seed media was prepared as

previously described Menacho-Melgar et al. (Romel Menacho-Melgar et al., n.d.) SM10++ and SM10 no phosphate media were prepared as described by Moreb et al.(Eirik A. Moreb et al. 2020) FGM3 media used in biolector studies is detailed in Supplemental Materials. Working antibiotic concentrations were as follows: kanamycin: 35 µg/mL, chloramphenicol: 35 µg/mL, zeocin: 100 µg/mL, blasticidin: 100 µg/mL, spectinomycin: 25 µg/mL, tetracycline:5 µg/mL.

Strains & Plasmids

Plasmid and strain information is given in Supplemental Materials. Sequences of oligonucleotides and synthetic linear DNA (Gblocks™) are given in Supplemental Materials, Tables S2 and S3, and they were obtained from Integrated DNA Technologies (IDT, Coralville, IA). Deletions were constructed with tet-sacB based selection and counterselection. (Li et al. 2013) C-terminal DAS+4 tag (with or without superfolder GFP tags) were added to chromosomal genes by direct integration and selected through integration of antibiotic resistance cassettes 3' of the gene. All strains were confirmed by PCR, agarose gel electrophoresis and confirmed by sequencing (Eton Biosciences, or Genewiz) using paired oligonucleotides, either flanking the entire region. The recombineering plasmid pSIM5 and the tet-sacB selection/counterselection marker cassette were kind gifts from Donald Court (NCI, https://redrecombineering.ncifcrf.gov/court-lab.html). Strain BW25113 was obtained from the Yale Genetic Stock Center (CGSC http://cgsc.biology.yale.edu/). Strain DLF_R002 was constructed as previously reported by Menacho-Melgar et al.(Romel Menacho-Melgar et al., n.d.) Strain DLFZ_0025 was constructed from DLF_R002 by first deleting the native *sspB* gene (using tet-sacB based selection and counterselection). Subsequently, the *cas3* gene was deleted (Luo et al. 2015b) and replaced with a low phosphate inducible sspB (using the *ugpB* gene promoter (Eirik Adim Moreb et al. 2020)) allele as well as a constitutive promoter to drive expression of the Cascade operon (again using tet-sacB based selection and counterselection). C-terminal DAS+4 tag modifications (with or without superfolder GFP tags) were added to the chromosome of DLF_Z0025 and its derivatives by direct integration and selected through integration of antibiotic resistance cassettes 3' of the gene.

Plasmids, pCDF-ev (Addgene #89596), pHCKan-yibDp-GFPuv (Addgene #127078) and pHCKan-yibDp-cimA3.7 (Addgene #134595) were constructed as previously reported.(Romel Menacho-Melgar et al., n.d.) Plasmids pCDF-mCherry1 (Addgene #87144) and pCDF-mCherry1 (Addgene #87145) were constructed from pCDF-ev by PCR and Gibson assembly with synthetic DNA encoding an mCherry open reading frame with out without a C-terminal DAS+4 degron tag along with a strong synthetic constitutive proD promoter previously reported by Davis et al. (Davis, Rubin, and Sauer 2011)

Gene silencing guides and guide arrays were expressed from a series of pCASCADE plasmids. The pCASCADE-control plasmid was prepared by swapping the pTet promoter in pcrRNA.Tet (a kind gift from C. Beisel) (Luo et al. 2015b) with an insulated low phosphate induced ugpB promoter. (Eirik Adim Moreb et al. 2020) In order to design CASCADE guide array, CASCADE PAM sites near the -35 or -10 box of the promoter of interest were identified, 30 bp at the 3' end of PAM site was selected as the guide sequence and cloned into pCASCADE plasmid using Q5 site-directed mutagenesis (NEB, MA) following manufacturer's protocol, with the modification that 5% v/v DMSO was added to the Q5 PCR reaction. PCR cycles were as follows: amplification involved an initial denaturation step at 98 °C for 30 second followed by cycling at 98 °C for 10 second, 72 °C for 30 second, and 72 °C for 1.5 min (the extension rate was 30 second/kb) for 25 cycles, then a final extension for 2 min at 72 °C. 2 µL of PCR mixture was used for 10 µL KLD reaction (NEB, MA), which proceeded under room temperature for 1 hour, after which, 1 µL KLD mixture was used for electroporation. The pCASCADE guide array plasmid (pCASCADE-G2Z) was prepared by sequentially amplifying complementary halves of each smaller guide plasmid by PCR, followed by subsequent DNA assembly as illustrated in Supplemental Materials. Primers used for pCASCADE assembly and gRNA sequences are provided in Supplemental Table S4. Additionally, all strains containing gRNA plasmids were routinely confirmed to assess gRNA stability via PCR as described below.

BioLector studies

Single colonies of each strain were inoculated into 5 mL LB with appropriate antibiotics and cultured at 37 °C, 220 rpm for 9 hours or until OD600 reached > 2. 500 µL of the culture

was inoculated into 10 mL SM10 medium with appropriate antibiotics, and cultured in a square shake flask (CAT#: 25-212, Genesee Scientific, Inc. San Diego, CA) at 37 °C, 220 rpm for 16 hours. Cells were pelleted by centrifugation and the culture density was normalized to OD600 = 5 using FGM3 media. Growth and fluorescence measurements were obtained in a Biolector (m2p labs,Baesweiler, Germany) using a high mass transfer FlowerPlate (CAT#: MTP-48-B, m2p-labs,Germany). 40 µL of the OD normalized culture was inoculated into 760 µL of FGM3 medium with appropriate antibiotics. Biolector settings were as follows: RFP gain=100, GFP gain=20, Biomass gain=20, shaking speed=1300 rpm, temperature=37 °C, humidity=85%. Every strain was analyzed in triplicate.

ELISAs

Quantification of proteins via C-terminal GFP tags was performed using a GFP quantification kit from AbCam (Cambridge, UK, product # ab171581) according to manufacturer's instructions.Briefly, samples were obtained from microfermentations as described above. Cells were harvested 24 hour post phosphate depletion, washed in water and lysed with the provided extraction buffer.

Guide RNA Stability Testing

The stability of guide RNA arrays was confirmed by colony PCR using the following 2 primers: gRNA-for: 5'-GGGAGACCACAACGG-3', gRNA-rev: 5'-CGCAGTCGAACGACCG-3', using 2X EconoTaq Master mix (Lucigen) in 10 µL PCR reactions consisting of 5µL of 2X EconoTaq Master mix (Lucigen) , 1uL of each primer (10µM), 3µL dH2O. A 98℃, 2 minute initial denaturation was followed by 35 cycles of 94℃, 30 seconds, 60℃ 30 seconds, and 72℃, 30 seconds and a final 72℃, 5 min final extension. PCR reactions were then run on agarose gels and band size compared to control PCR reactions using purified plasmid DNA as a template. Guide protospacer loss occurred when guide array size was smaller than expected, indicating the loss of one or more protospacers.

Fermentations

Minimal media microfermentations were performed as previously reported.(Eirik Adim Moreb et al. 2020) For microfermentations where paraquat induction was used, paraquat was added for 1 hour prior to phosphate depletion and subsequently removed during the cell wash step used to deplete phosphate in the media. 1L fermentations in instrumented bioreactors were also performed as previously reported, (Menacho-Melgar et al. 2020) with slight modifications to the glucose feeding profiles, which were a function of strain and process. Generally, feeding was increased to enable excess residual glucose to ensure production rates were not feed limited. Glucose feeding was as follows. For 10 gCDW/L fermentations, starting batch glucose concentration was 25 g/L. A constant concentrated sterile filtered glucose feed (500 g/L) was added to the tanks at 1.5 g/h when cells entered mid-exponential growth. For 25 gCDW/L fermentations, starting batch glucose concentration was 25 g/L. Concentrated sterile filtered glucose feed (500 g/L) was added to the tanks at an initial rate of 9 g/h when cells entered mid-exponential growth. This rate was then increased exponentially, doubling every 1.083 hours (65 min) until 40 g total glucose had been added, after which the feed was maintained at 1.75g/hr.

Production of Isotopically Labelled Metabolites.

C^{13} pyruvate (CLM-1082-PK) and C^{13} D-glucose (U-13C6, 99%) were purchased from Cambridge Isotope Laboratories, Inc. (Tewksbury, MA). Isotopically labelled citramalate was produced in two stage minimal media shake flask studies , mimicking microfermentations, using strain DLF_Z0044 expressing cimA3.7. Briefly, 20 mL cultures of SM10++ media (Menacho-Melgar et al. 2020) were inoculated with the strain which was grown overnight at 37 Celsius, shaking at 150 rpm in baffled 250 mL Erlenmyer shake flasks. After 16 hrs of growth cells were harvested by centrifugation washed and resuspended in 20mL of SM10 minimal media (lacking phosphate) (Menacho-Melgar et al. 2020) where glucose was replaced with C^{13} labelled glucose. Cultures were grown for 25 hrs at 37 Celsius, shaking at 150 rpm, after which cells were removed by centrifugation, and the spent media filter sterilized prior to use as an internal standard.

Analytical Methods

Cell dry weights: The OD/cell dry weight correlation coefficient (1 OD(600nm) = 0.35 gCDW/L, as determined by Menacho-Melgar et al. was used in this work. (Menacho-Melgar et al. 2020)

Glucose and Organic Acid Quantification: Two methods were used for glucose and organic acid quantification. First, a UPLC-RI method was developed for the simultaneous quantification of glucose, citramalate, acetic acid, pyruvate, citraconate, citrate and other organic acids including lactate, succinate, fumarate, malate, and mevalonate. Chromatographic separation was performed using a Rezex Fast Acid Analysis HPLC Column (100 x 7.8 mm, 9 µm particle size; CAT#: #1250100, Bio-Rad Laboratories, Inc., Hercules, CA) at 55 ℃. 5 mM sulfuric acid was used as the isocratic eluent, with a flow rate of XmL/min. Sample injection volume was 10 µL. Second, quantification was performed using a Bio-Rad Fast Acid Analysis HPLC Column (100 x 7.8 mm, 9 µm particle size; CAT#: #1250100, Bio-Rad Laboratories, Inc., Hercules, CA) at 65 ℃. 10 mM sulfuric acid was used as the eluent, with an isocratic flow rate of 0.3mL/min. In both methods, sample injection volume was 10 µL and chromatography and detection were accomplished using a Waters Acquity H-Class UPLC integrated with a Waters 2414 Refractive Index (RI) detector (Waters Corp., Milford, MA. USA). Samples were diluted as needed to be within the accurate linear range. Dilution was performed using ultrapure water.

Organic acid Quantification via RapidFire-qTOF-MS: Micro-fermentation samples (as well as a confirmatory subset of samples from bioreactors) were centrifuged to remove cells. Broth was diluted 100 fold in water to a final volume of 20 µL. To this either a final concentration of 10 mg/L of C13 pyruvate was added or 2 uL of broth containing C13 labelled citramalate was added. The final sample was injected onto a HILIC (type H1 or the equivalent H6) RapidFire™ cartridge (Agilent Technologies, Santa Clara, CA). Injections were loaded on the cartridge with 95% hexane, 5% isopropanol for 3000 ms after a 600ms aspiration, at a flow rate of 1.0 mL/min. After loading, the cartridge was washed with isopropanol for 2000ms, at a flow rate of 1.0 mL/min. Elution was carried out for 8000 ms with 50% water/ 50% methanol with 0.2% acetic

acid and 0.5 uM $(NH_4)_3PO_4$, (Spalding et al. 2018) at a flow rate of 1.0 mL/min. Column equilibration was performed for 4000ms. The qTOF was tuned in the mass range of 50-250 m/z in fragile ion, negative ESI mode. Settings during detection were as follows: drying gas: 250C at a flow rate of 13L/minute, sheath gas: 400 C at a flow rate of 12L/minute , nebulizer pressure: 35 psi, Fragmenter voltage: 100 V, skimmer voltage: 65 V, nozzle voltage: 2000 V, capillary voltage: 3500V. The acquisition rate was 1 spectra/second.

Acknowledgements

We would like to acknowledge the following support: NSF EAGER: #1445726, DARPA# HR0011-14-C-0075, ONR YIP #N00014-16-1-2558, DOE EERE grant #EE0007563 and financial support from DMC Biotechnologies, Inc. Additionally, we would also like to thank Michelle Luo and Chase Beisel for the kind gift of pcrRNA.Tet and support in implementation of Cascade based gene silencing.

Author contributions

S. Li constructed plasmids and strains, performed microfermentations and fermentation studies and related analyses. Z. Ye constructed plasmids and strains, developed microfermetnation protocols, performed microfermentations and fermentation studies and related analyses. E.A. Moreb performed microfermentations and J. Lebeau performed ELISAs and fermentations. M.D. Lynch designed and analyzed experiments, constructed strains and performed ELISAs, and analytical analyses. All authors wrote revised and edited the manuscript.

Conflicts of Interest

M.D. Lynch and Z. Ye have a financial interest in DMC Biotechnologies, Inc. M.D. Lynch, and E.A. Moreb have a financial interest in Roke Biotechnologies, Inc.

References

Akhtar, M. Kalim, M. Kalim Akhtar, and Patrik R. Jones. 2009. "Construction of a Synthetic YdbK-Dependent pyruvate:H2 Pathway in Escherichia Coli BL21(DE3)." *Metabolic Engineering*. https://doi.org/10.1016/j.ymben.2009.01.002.

Atsumi, Shota, and James C. Liao. 2008. "Directed Evolution of Methanococcus Jannaschii Citramalate Synthase for Biosynthesis of 1-Propanol and 1-Butanol by Escherichia Coli." *Applied and Environmental Microbiology* 74 (24): 7802–8.

Blaschkowski, Hans P., Joachim Knappe, Monika Ludwig-Festl, and Gabriele Neuer. 1982. "Routes of Flavodoxin and Ferredoxin Reduction in Escherichia Coli: CoA-Acylating Pyruvate: Flavodoxin and NADPH: Flavodoxin Oxidoreductases Participating in the Activation of Pyruvate Formate-Lyase." *European Journal of Biochemistry / FEBS* 123 (3): 563–69.

Bordbar, Aarash, Jonathan M. Monk, Zachary A. King, and Bernhard O. Palsson. 2014. "Constraint-Based Models Predict Metabolic and Associated Cellular Functions." *Nature Reviews. Genetics* 15 (2): 107–20.

Brockman, Irene M., and Kristala L. J. Prather. 2015a. "Dynamic Knockdown of E. Coli Central Metabolism for Redirecting Fluxes of Primary Metabolites." *Metabolic Engineering* 28 (March): 104–13.

———. 2015b. "Dynamic Metabolic Engineering: New Strategies for Developing Responsive Cell Factories." *Biotechnology Journal* 10 (9): 1360–69.

Brouns, Stan J. J., Matthijs M. Jore, Magnus Lundgren, Edze R. Westra, Rik J. H. Slijkhuis, Ambrosius P. L. Snijders, Mark J. Dickman, Kira S. Makarova, Eugene V. Koonin, and John van der Oost. 2008. "Small CRISPR RNAs Guide Antiviral Defense in Prokaryotes." *Science* 321 (5891): 960–64.

Burgard, Anthony P., Priti Pharkya, and Costas D. Maranas. 2003. "Optknock: A Bilevel Programming Framework for Identifying Gene Knockout Strategies for Microbial Strain Optimization." *Biotechnology and Bioengineering* 84 (6): 647–57.

Burg, J. M., C. B. Cooper, Z. Ye, B. R. Reed, and E. A. Moreb. 2016. "Large-Scale Bioprocess Competitiveness: The Potential of Dynamic Metabolic Control in Two-Stage Fermentations." *Current Opinion in*. https://www.sciencedirect.com/science/article/pii/S2211339816300703.

Christodoulou, Dimitris, Hannes Link, Tobias Fuhrer, Karl Kochanowski, Luca Gerosa, and Uwe Sauer. 2018. "Reserve Flux Capacity in the Pentose Phosphate Pathway Enables Escherichia Coli's Rapid Response to Oxidative Stress." *Cell Systems* 6 (5): 569–78.e7.

Chubukov, Victor, and Uwe Sauer. 2014. "Environmental Dependence of Stationary-Phase Metabolism in Bacillus Subtilis and Escherichia Coli." *Applied and Environmental Microbiology* 80 (9): 2901–9.

David, Florian, Jens Nielsen, and Verena Siewers. 2016. "Flux Control at the Malonyl-CoA Node through Hierarchical Dynamic Pathway Regulation in Saccharomyces Cerevisiae." *ACS Synthetic Biology* 5 (3): 224–33.

Davis, Joseph H., Adam J. Rubin, and Robert T. Sauer. 2011. "Design, Construction and Characterization of a Set of Insulated Bacterial Promoters." *Nucleic Acids Research* 39 (3): 1131–41.

Ding, Wentao, Yang Zhang, and Shuobo Shi. 2020. "Development and Application of CRISPR/Cas in Microbial Biotechnology." *Frontiers in Bioengineering and Biotechnology* 8: 711.

Doucette, Christopher D., David J. Schwab, Ned S. Wingreen, and Joshua D. Rabinowitz. 2011. "α-Ketoglutarate Coordinates Carbon and Nitrogen Utilization via Enzyme I Inhibition." *Nature Chemical Biology* 7 (12): 894–901.

Eremina, N. S. 2010. “Overexpression of ydbKencoding Putative Pyruvate Synthase Improves L-Valine Production and Aerobic Growth on Ethanol Media by an Escherichia Coli Strain Carrying an Oxygen-Resistant Alcohol Dehydrogenase.” *J. Microbial Biochem. Technol.* 2: 77–83.

Fàbrega, Anna, Judah L. Rosner, Robert G. Martin, Mar Solé, and Jordi Vila. 2012. “SoxS-Dependent Coregulation of ompN and ydbK in a Multidrug-Resistant Escherichia Coli Strain.” *FEMS Microbiology Letters* 332 (1): 61–67.

Gardner, T. S., C. R. Cantor, and J. J. Collins. 2000. “Construction of a Genetic Toggle Switch in Escherichia Coli.” *Nature* 403 (6767): 339–42.

Gaudu, Philippe, Sarah Dubrac, and Danièle Touati. 2000. “Activation of SoxR by Overproduction of Desulfoferrodoxin: Multiple Ways To Induce the soxRSRegulon.” *Journal of Bacteriology* 182 (6): 1761–63.

Giró, Mariana, Néstor Carrillo, and Adriana R. Krapp. 2006. “Glucose-6-Phosphate Dehydrogenase and Ferredoxin-NADP(H) Reductase Contribute to Damage Repair during the soxRS Response of Escherichia Coli.” *Microbiology*. https://doi.org/10.1099/mic.0.28612-0.

Greenberg, J. T., P. Monach, J. H. Chou, P. D. Josephy, and B. Demple. 1990. “Positive Control of a Global Antioxidant Defense Regulon Activated by Superoxide-Generating Agents in Escherichia Coli.” *Proceedings of the National Academy of Sciences of the United States of America* 87 (16): 6181–85.

Griffith, Kevin L., and Richard E. Wolf. 2001. “Systematic Mutagenesis of the DNA Binding Sites for SoxS in the Escherichia Coli Zwf and Fpr Promoters: Identifying Nucleotides Required for DNA Binding and Transcription Activation.” *Molecular Microbiology*. https://doi.org/10.1046/j.1365-2958.2001.02568.x.

Grünenfelder, B., G. Rummel, J. Vohradsky, D. Röder, H. Langen, and U. Jenal. 2001. “Proteomic Analysis of the Bacterial Cell Cycle.” *Proceedings of the National Academy of Sciences of the United States of America* 98 (8): 4681–86.

Hennig, J., G. Kern, H. Neef, M. Spinka, H. Bisswanger, and G. Hübner. 1997. “Molecular Mechanism of Regulation of the Pyruvate Dehydrogenase Complex from E. Coli.” *Biochemistry* 36 (50): 15772–79.

Hintsche, Marius, and Stefan Klumpp. 2013. “Dilution and the Theoretical Description of Growth-Rate Dependent Gene Expression.” *Journal of Biological Engineering* 7 (1): 22.

Howell, D. M., H. Xu, and R. H. White. 1999. “(R)-Citramalate Synthase in Methanogenic Archaea.” *Journal of Bacteriology* 181 (1): 331–33.

Huber, R., S. Roth, N. Rahmen, and J. Buchs. 2011. “Utilizing High-Throughput Experimentation to Enhance Specific Productivity of an E.coli T7 Expression System by Phosphate Limitation.” *BMC Biotechnology* 11: 22.

Huergo, Luciano F., and Ray Dixon. 2015. “The Emergence of 2-Oxoglutarate as a Master Regulator Metabolite.” *Microbiology and Molecular Biology Reviews: MMBR* 79 (4): 419–35.

Jarboe, Laura R., Xueli Zhang, Xuan Wang, Jonathan C. Moore, K. T. Shanmugam, and Lonnie O. Ingram. 2010. “Metabolic Engineering for Production of Biorenewable Fuels and Chemicals: Contributions of Synthetic Biology.” *Journal of Biomedicine & Biotechnology* 2010 (April): 761042.

Kildegaard, K. R., L. R. R. Tramontin, K. Chekina, and M. Li. 2019. “CRISPR/Cas9‐RNA

Interference System for Combinatorial Metabolic Engineering of Saccharomyces Cerevisiae." *Yeast* . https://onlinelibrary.wiley.com/doi/abs/10.1002/yea.3390.

Kok, A. de, A. F. Hengeveld, A. Martin, and A. H. Westphal. 1998. "The Pyruvate Dehydrogenase Multi-Enzyme Complex from Gram-Negative Bacteria." *Biochimica et Biophysica Acta* 1385 (2): 353–66.

Lalwani, Makoto A., Evan M. Zhao, and José L. Avalos. 2018. "Current and Future Modalities of Dynamic Control in Metabolic Engineering." *Current Opinion in Biotechnology* 52 (August): 56–65.

Lebeau, Juliana, John P. Efromson, and Michael D. Lynch. 2020. "A Review of the Biotechnological Production of Methacrylic Acid." *Frontiers in Bioengineering and Biotechnology* 8: 207.

Lee, Jeong Wook, Dokyun Na, Jong Myoung Park, Joungmin Lee, Sol Choi, and Sang Yup Lee. 2012. "Systems Metabolic Engineering of Microorganisms for Natural and Non-Natural Chemicals." *Nature Chemical Biology* 8 (6): 536–46.

Li, Xin-Tian, Lynn C. Thomason, James A. Sawitzke, Nina Costantino, and Donald L. Court. 2013. "Positive and Negative Selection Using the tetA-sacB Cassette: Recombineering and P1 Transduction in Escherichia Coli." *Nucleic Acids Research* 41 (22): e204.

Luo, Michelle L., Adam S. Mullis, Ryan T. Leenay, and Chase L. Beisel. 2015a. "Repurposing Endogenous Type I CRISPR-Cas Systems for Programmable Gene Repression." *Nucleic Acids Research*. https://doi.org/10.1093/nar/gku971.

———. 2015b. "Repurposing Endogenous Type I CRISPR-Cas Systems for Programmable Gene Repression." *Nucleic Acids Research* 43 (1): 674–81.

Lynch, Michael D. 2016. "Into New Territory: Improved Microbial Synthesis through Engineering of the Essential Metabolic Network." *Current Opinion in Biotechnology* 38 (April): 106–11.

Maury, Jérôme, Soumya Kannan, Niels B. Jensen, Fredrik K. Öberg, Kanchana R. Kildegaard, Jochen Forster, Jens Nielsen, Christopher T. Workman, and Irina Borodina. 2018. "Glucose-Dependent Promoters for Dynamic Regulation of Metabolic Pathways." *Frontiers in Bioengineering and Biotechnology* 6 (May): 63.

McGinness, Kathleen E., Tania A. Baker, and Robert T. Sauer. 2006. "Engineering Controllable Protein Degradation." *Molecular Cell* 22 (5): 701–7.

Menacho-Melgar, R., E. A. Moreb, and J. P. Efromson. 2020. "Improved, Two-Stage Protein Expression and Purification via Autoinduction of Both Autolysis and Auto DNA/RNA Hydrolysis Conferred by Phage Lysozyme and DNA/RNA …." *bioRxiv*. https://www.biorxiv.org/content/10.1101/2020.01.09.900753v1.abstract.

Menacho-Melgar, Romel, Zhixia Ye, Eirik A. Moreb, Tian Yang, John P. Efromson, John S. Decker, and Michael D. Lynch. n.d. "Improved, Scalable, Two-Stage, Autoinduction of Recombinant Protein Expression in E. Coli Utilizing Phosphate Depletion." https://doi.org/10.1101/820787.

Menacho‐Melgar, Romel, Zhixia Ye, Eirik A. Moreb, Tian Yang, John P. Efromson, John S. Decker, Ruixin Wang, and Michael D. Lynch. 2020. "Scalable, Two‐stage, Autoinduction of Recombinant Protein Expression in E. Coli Utilizing Phosphate Depletion." *Biotechnology and Bioengineering* 26 (June): 44.

Moreb, Eirik Adim, Zhixia Ye, John P. Efromson, Jennifer N. Hennigan, Romel Menacho-Melgar, and Michael D. Lynch. 2020. "Media Robustness and Scalability of

Phosphate Regulated Promoters Useful for Two-Stage Autoinduction in E. Coli." *ACS Synthetic Biology*. https://doi.org/10.1021/acssynbio.0c00182.

Moreb, Eirik A., Zhixia Ye, John P. Efromson, Jennifer N. Hennigan, Romel Menacho-Melgar, and Michael D. Lynch. 2020. "Robustness Testing and Scalability of Phosphate Regulated Promoters Useful for Two-Stage Autoinduction in E. Coli." https://doi.org/10.1021/acssynbio.0c00182.

Nakayama, Takayuki, Shin-Ichiro Yonekura, Shuji Yonei, and Qiu-Mei Zhang-Akiyama. 2013. "*Escherichia Coli* Pyruvate:flavodoxin Oxidoreductase, YdbK - Regulation of Expression and Biological Roles in Protection against Oxidative Stress." *Genes & Genetic Systems*. https://doi.org/10.1266/ggs.88.175.

Parimi, Naga Sirisha, Ian A. Durie, Xianghao Wu, Afaq M. M. Niyas, and Mark A. Eiteman. 2017. "Eliminating Acetate Formation Improves Citramalate Production by Metabolically Engineered Escherichia Coli." *Microbial Cell Factories* 16 (1): 114.

Pédelacq, Jean-Denis, Stéphanie Cabantous, Timothy Tran, Thomas C. Terwilliger, and Geoffrey S. Waldo. 2006. "Engineering and Characterization of a Superfolder Green Fluorescent Protein." *Nature Biotechnology* 24 (1): 79–88.

Qi, Lei S., Matthew H. Larson, Luke A. Gilbert, Jennifer A. Doudna, Jonathan S. Weissman, Adam P. Arkin, and Wendell A. Lim. 2013. "Repurposing CRISPR as an RNA-Guided Platform for Sequence-Specific Control of Gene Expression." *Cell* 152 (5): 1173–83.

Rabinowitz, Joshua D., and Thomas J. Silhavy. 2013. "Systems Biology: Metabolite Turns Master Regulator." *Nature*.

Solomon, Kevin V., Tarielle M. Sanders, and Kristala L. J. Prather. 2012. "A Dynamic Metabolite Valve for the Control of Central Carbon Metabolism." *Metabolic Engineering*. https://doi.org/10.1016/j.ymben.2012.08.006.

Soma, Yuki, Keigo Tsuruno, Masaru Wada, Atsushi Yokota, and Taizo Hanai. 2014. "Metabolic Flux Redirection from a Central Metabolic Pathway toward a Synthetic Pathway Using a Metabolic Toggle Switch." *Metabolic Engineering* 23 (May): 175–84.

Spalding, Jonathan L., Fuad J. Naser, Nathaniel G. Mahieu, Stephen L. Johnson, and Gary J. Patti. 2018. "Trace Phosphate Improves ZIC-pHILIC Peak Shape, Sensitivity, and Coverage for Untargeted Metabolomics." *Journal of Proteome Research* 17 (10): 3537–46.

Venayak, Naveen, Axel von Kamp, Steffen Klamt, and Radhakrishnan Mahadevan. 2018. "MoVE Identifies Metabolic Valves to Switch between Phenotypic States." *Nature Communications* 9 (1): 5332.

Webb, Joseph P., S. Alison Arnold, Scott Baxter, Stephen J. Hall, Graham Eastham, and Gill Stephens. 2018. "Efficient Bio-Production of Citramalate Using an Engineered Escherichia Coli Strain." *Microbiology* 164 (2): 133–41.

Webb, Joseph, Vicki Springthorpe, Luca Rossoni, David-Paul Minde, Swen Langer, Heather Walker, Amias Alstrom-Moore, et al. 2019. "Systems Analyses Reveal the Resilience of Escherichia Coli Physiology during Accumulation and Export of the Nonnative Organic Acid Citramalate." *mSystems* 4 (4). https://doi.org/10.1128/mSystems.00187-19.

Wu, Xianghao, and Mark A. Eiteman. 2016. "Production of Citramalate by Metabolically Engineered Escherichia Coli." *Biotechnology and Bioengineering* 113 (12): 2670–75.

Xu, Peng, Lingyun Li, Fuming Zhang, Gregory Stephanopoulos, and Mattheos Koffas. 2014. "Improving Fatty Acids Production by Engineering Dynamic Pathway Regulation and Metabolic Control." *Proceedings of the National Academy of Sciences of the United States*

of America 111 (31): 11299–304.

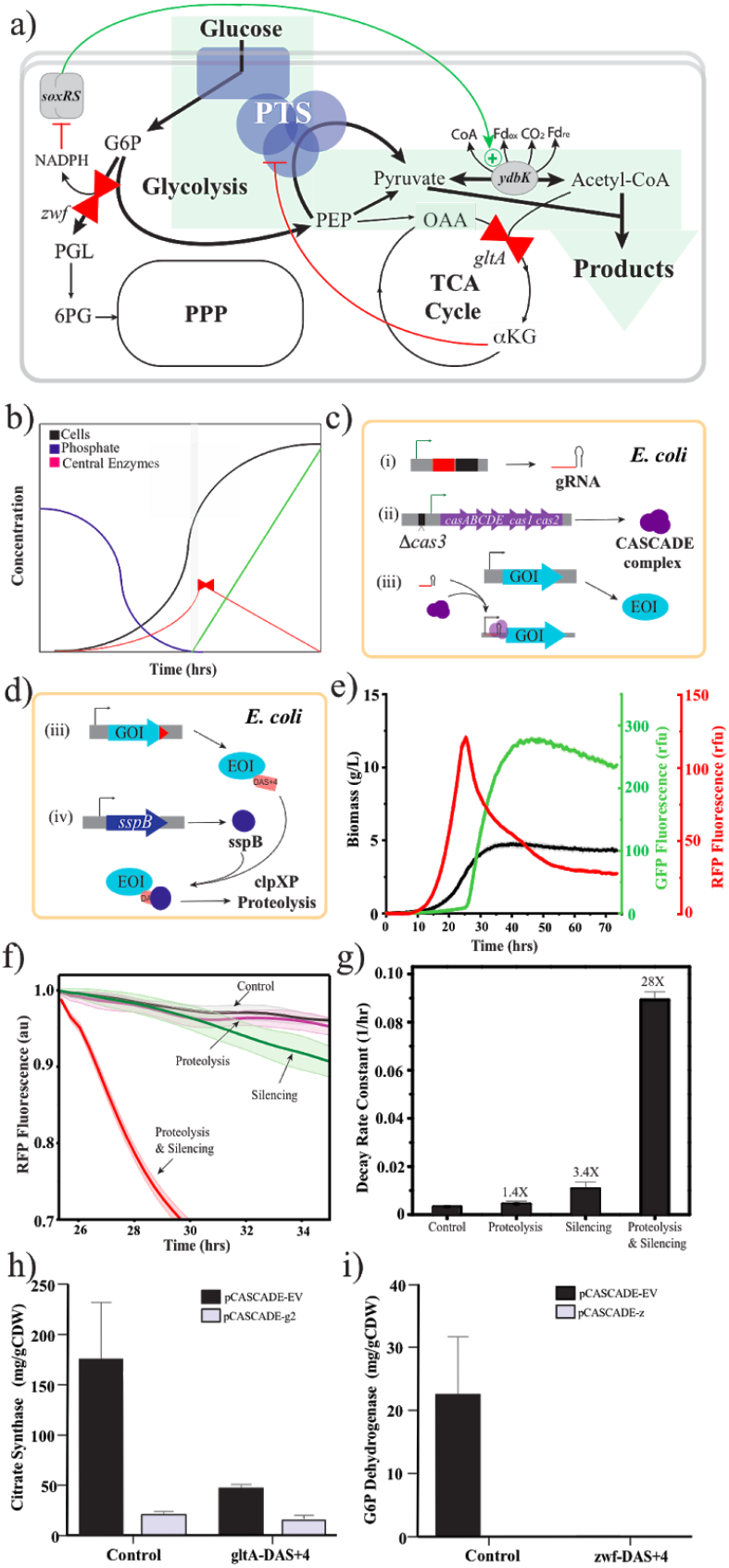
a)
Glucose
PTS
soxRS
NADPH
G6P
Glycolysis
zwf
PGL
6PG
PPP
PEP
Pyruvate
CoA
Fdox
CO2
Fdre
ydbK
Acetyl-CoA
OAA
gltA
TCA
Cycle
αKG
Products
b)
Cells
Phosphate
Central Enzymes
Concentration
Time (hrs)
c)
E. coli
(i)
gRNA
(ii)
casABCDE cas1 cas2
Δcas3
CASCADE
complex
(iii)
GOI
EOI
d)
E. coli
(iii)
GOI
EOI
DAS+4
(iv)
sspB
sspB
EOI
clpXP
Proteolysis
e)
Biomass (g/L)
GFP Fluorescence (rfu)
RFP Fluorescence (rfu)
Time (hrs)
f)
RFP Fluorescence (au)
Control
Proteolysis
Silencing
Proteolysis
& Silencing
Time (hrs)
g)
Decay Rate Constant (1/hr)
28X
3.4X
1.4X
Control
Proteolysis
Silencing
Proteolysis
& Silencing
h)
Citrate Synthase (mg/gCDW)
pCASCADE-EV
pCASCADE-g2
Control
gltA-DAS+4
i)
G6P Dehydrogenase (mg/gCDW)
pCASCADE-EV
pCASCADE-z
Control
zwf-DAS+4

Figure 1: (a) Two-stage dynamic control over feedback regulation of central metabolism improves stationary phase sugar uptake and acetyl-CoA flux. Metabolic valves (red double triangles) dynamically reduce levels off Zwf (glucose-6-phosphate dehydrogenase) and GltA (citrate synthase). Reduced flux through the TCA cycle reduces αKG levels alleviating feedback inhibition of PTS dependent glucose uptake, improving glycolytic fluxes and pyruvate production. Reduced flux Zwf reduces NADPH levels activating the SoxRS oxidative stress response regulation and increasing expression and activity of pyruvate ferredoxin oxidoreductase improving pyruvate oxidation and acetyl-CoA flux. (b) Time course of two stage dynamic metabolic control upon phosphate depletion Biomass levels accumulate and consume a limiting nutrient (in this case inorganic phosphate), which when depleted triggers entry into a productive stationary phase, levels of key enzymes are dynamically reduced with synthetic metabolic valves (red) (c & d). Synthetic metabolic valves utilizing CRISPRi based gene silencing and/or controlled proteolysis. (c) Array of silencing guides can be used to silencing target multiple genes of interest (GOI). This involves the inducible expression of one or many guide RNAs as well as expression of the modified native Cascade system wherein the cas3 nuclease is deleted. The gRNA/Cascade complex binds to target sequences in the promoter region and silences transcription. (d) C-terminal DAS+4 tags are added to enzymes of interest (EOI) through chromosomal modification, they can be inducibly degraded by the clpXP protease in the presence of an inducible sspB chaperone. (e) Dynamic control over protein levels in *E. coli* using inducible proteolysis and CRISPRi silencing. As cells grow phosphate is depleted, cells "turn off" mCherry and "turn on" GFPuv. Shaded areas represent one standard deviation from the mean, n=3. (f) The relative impact of proteolysis and gene silencing alone and in combination on mCherry degradation, (g) mCherry decays rates. (h & i) Dynamic Control over the levels of the central metabolic enzymes. The impact of silencing (pCASCADE) and proteolysis (DAS+4 tags) on protein levels were evaluated alone and in combination (h) GltA (citrate synthase), and (i) Zwf (glucose-6-phosphate dehydrogenase). In all cases chromosomal genes were tagged with a C-terminal sfGFP. Protein levels were measured by ELISA, 24 hour post induction by phosphate depletion in microfermentations. Abbreviations: PTS: phosphotransferase transport system, PPP: pentose phosphate pathway, TCA: tricarboxylic acid, G6P: glucose-6-phosphate, 6-PGL: 6-phosphogluconolactone, 6PG: 6-phosphogluconate, PEP: phosphoenolpyruvate, Fd: ferredoxin, CoA: coenzyme A, OAA: oxaloacetate, αKG: α-ketoglutarate.

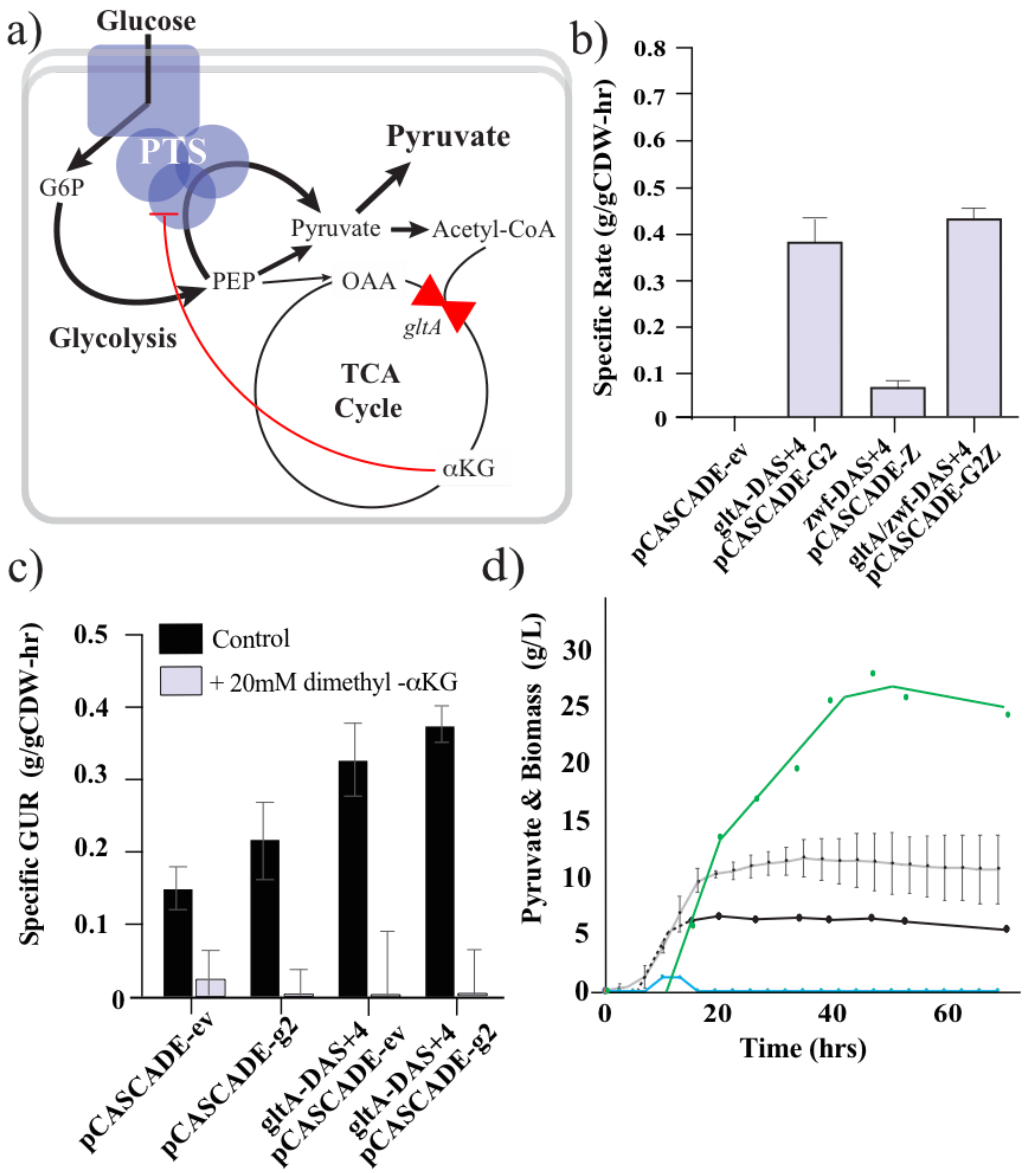

Figure 2: a) Dynamic reduction in GltA reduces αKG pools and alleviates αKG mediated inhibition of PTS-dependent glucose uptake (specifically, PtsI), improving glucose uptake rates, glycolytic fluxes and pyruvate production. b) The impact of dynamic control over GltA and Zwf levels on pyruvate production in minimal media microfermetnations. c) The impact of dynamic control over GltA and Zwf levels and dimethyl-αKG supplementation on glucose uptake rates in microfermentations. (d) Pyruvate and biomass production were measured for the control strain and the "G" valve strain. The control strain's biomass (gray) and pyruvate production (blue), as well as the "G" valve strain's biomass (black) and pyruvate production (green) are plotted as a function of time. Dashed line represents extrapolated growth due to missed samples.

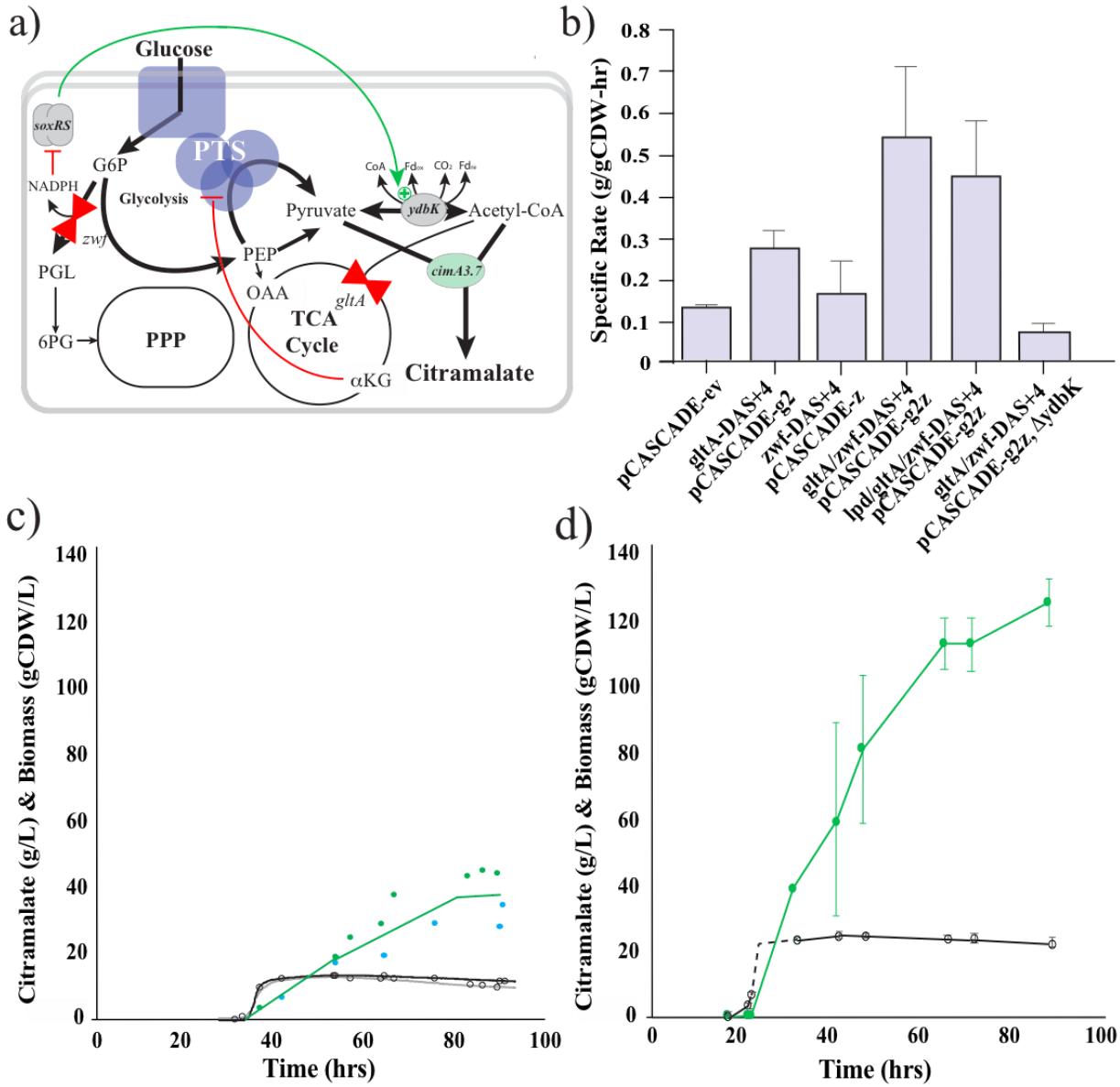

Figure 3: a) Dynamic reduction in Zwf levels activates the SoxRS regulon and increases activity of the pyruvate-ferredoxin oxidoreductase (Pfo, *ydbK*) improving acetyl-CoA fluxes and citramalate production. b) The impact of dynamic control over GltA and Zwf levels on citramalate production in minimal media microfermetnations. Additionally, the proteolytic degradation of Lpd (lpd-DAS+4, a subunit of the pyruvate dehydrogenase multienzyme complex) and a deletion in *ydbK* were assessed in the "GZ" valve background. (c & d) Citramalate and biomass production were measured for the control strain (c) and the "GZ" valve strain (d). (c) Duplicate runs, biomass levels in gray and black, citramalate titers in green and blue. (d) The average of triplicate runs, biomass black and citramalate green. Dashed line represents extrapolated growth due to missed samples.